



# Application of carboxymethylcellulose in combination with essential oils nano-emulsions edible coating for the preservation of kiwifruit



Shahzad Zafar Iqbal <sup>a,\*</sup>, Ali Haider <sup>a</sup>, Fazal ur Rehman <sup>a</sup>, Guihua Cui <sup>b</sup>, Muhammad Waseem <sup>a</sup>, Munawar Iqbal <sup>c</sup>, Amin Mousavi Khaneghah <sup>d</sup>

<sup>a</sup> Food Safety and Toxicology Lab, Department of Applied Chemistry, Government College University, Faisalabad 38000, Punjab, Pakistan

<sup>b</sup> Department of Pharmacy, Jilin Medical University, Jilin 132013, China

<sup>c</sup> Department of Chemistry, Division of Science and Technology, University of Education, Lahore, Pakistan

<sup>d</sup> Fruit and Vegetable Product Technology, Prof. Waclaw Dąbrowski Institute of Agricultural and Food Biotechnology – State Research Institute, 36 Rakowiecka F St., 02-532 Warsaw, Poland

## ARTICLE INFO

### Keywords:

Nano-emulsions  
Carboxymethyl cellulose  
Essential oils  
Preservation  
Shelf-life  
Kiwifruit

## ABSTRACT

The present research investigates the effectiveness of nano-emulsified coatings (C-1, C-2, and C-3) in preserving the kiwifruit at a temperature of  $10 \pm 2^\circ\text{C}$  with 90–95 % relative humidity (RH) for 30 days. The nano-emulsions were prepared from varied carboxymethyl cellulose (CMC) concentrations with different combinations of essential oils such as thyme, clove, and cardamom. Dynamic light scattering investigation with Zeta Sizer revealed that C-1, C-2, and C-3 nano-emulsions have nano sizes of  $81.3 \pm 2.3$ ,  $115.3 \pm 4.2$ , and  $63.2 \pm 3.2$  nm, respectively. The scanning electron microscopy images showed that the nanoemulsion of C-1 had homogenous spherical globules, C-2 had voids, and C-3 showed a non-porous structure with uniform dispersion. The X-ray diffraction analysis indicated that C-1, C-2, and C-3 nano-emulsion exhibited distinct crystallinity and peaks. The nano-emulsion C-1 had reduced crystallinity, while C-2 had lower intensity peaks, and C-3 had increased crystallinity. The results documented that compared to control kiwifruit samples, the samples coated with C-3 nano-emulsion have decreased weight loss, decay incidence, soluble solids, maturity index activity, ethylene production, total bacterial count, and increased titratable acid, and firmness attributes. The results of current research are promising and would be applicable in utilization in industrial applications.

## 1. Introduction

Kiwifruit (*Actinidia deliciosa*) is classified as a typical respiration climacteric fruit. This fruit variety is renowned for its exceptional nutritive value, earning it the esteemed title of the “King of fruits” [1]. However, it is noteworthy that kiwifruit exhibits a high susceptibility to decay, significantly impacting their nutritional composition and overall commercial viability throughout the storage and transportation processes. The key determinants that substantially influence the preservation of kiwifruit postharvest are the concentration of ethylene and the total count of bacteria [2]. To date, the methodologies employed for the storage and preservation of kiwifruit encompass a range of techniques, such as low-temperature treatment, coating treatment, modified atmosphere packaging, high-intensity ultrasound, nanoemulsions, and oxalic acid treatment, among others [2–8]. While implementing various preservation techniques has demonstrated the potential to extend the

persistence and adhere to the overall quality of kiwifruit, it is necessary to acknowledge the existence of certain challenges in their practical acceptance and widespread utilization. The potential impact of chemical preservation methods on consumer health has yet to be conclusively established. Pursuing a secure and efficient methodology to augment the acquired commercial caliber of kiwifruit is of utmost urgency for researchers [1].

Edible coatings often comprise polysaccharides, proteins, lipids, or a combination thereof [9]. Carboxymethyl cellulose (CMC) is a commonly used polysaccharide obtained from cellulose. It mainly manufactures films and coatings [10,11]. Researchers have employed carboxymethyl cellulose (CMC) as a protective layer to extend the storage duration of perishable food items such as avocados [12], peaches, and pears [13,14], including fresh tomatoes [15]. Cellulose stability makes it a promising food preservation preference, particularly for nanoemulsions. Cellulose nanocrystals (CNC) were used as stabilizers and fillers to

\* Corresponding author.

E-mail addresses: [shahzad10542005@yahoo.com](mailto:shahzad10542005@yahoo.com), [shahzad@gcuf.edu.pk](mailto:shahzad@gcuf.edu.pk) (S.Z. Iqbal).

enhance the stability of beta-galactosidase (b-gal) loaded low molecular weight (LMW) b-chitosan nanoparticles (b-CS NPs) and improve enzyme activity and in vitro release control [16]. Another study demonstrated that CNC- and GSS-stabilized high internal phase emulsions (HIPEs) stabilized oregano essential oil (OEO) without surfactants. HIPEs exhibited the smallest droplets and best month-long storage stability at 0.4 wt. CNC. The study found that CNC can stabilize and emulsify HIPEs to form gel-like, tunable microstructure and rheology [17].

Integrating bioactive components, such as antioxidants and anti-bacterial substances, is a recent development in edible composite films and coatings [18]. Essential oils (EO) as natural antibacterial agents in edible coatings have recently gained considerable attention for preserving food and extending its shelf life [19]. EO has a positive impact on food's visual appeal [20–22]. Thyme, clove, and cardamom essential oils are frequently incorporated into food formulations for their appealing aroma and diverse health benefits, including antioxidant, antimicrobial, chemopreventive, anti-cancer, and anti-inflammatory properties [23,24]. Thyme essential oil, with major constituents like thymol, has demonstrated antioxidant, anti-inflammatory, antibacterial, antimicrobial, antifungal, antiparasitic, immunological, and anticancer effects [25]. Clove oil, primarily composed of eugenol, a potent antioxidant, helps mitigate free radical activity [26]. Cardamom essential oil, rich in oxygenated monoterpenes like 1,8-cineole, exhibits key antioxidant properties [23]. Combined essential oils may show enhanced antimicrobial and antioxidant activities compared to individual components at similar concentrations, potentially yielding a synergistic effect due to the complementary actions of bioactive compounds in each oil. Studies suggest that such combinations can result in overall activity greater than the sum of individual effects, emphasizing the potential for synergistic benefits [27,28]. Significant loss of EO has been reported as another problem during coating and storage processes (Ju et al., 2019). To address these limitations and enhance the antimicrobial efficacy of essential oils (EO), scientists have devised an edible coating method utilizing a biopolymer-based nanoemulsion loaded with EO. This nanoform can augment EO's physicochemical and biological properties through an increase in surface area [29]. In addition, nanoemulsions possess the advantages of transparency and cost-effectiveness, effectively masking the taste and odor of the core substance. As a result, the impact on the sensory properties of food is minimized [30]. Nanoemulsion-based antimicrobial packaging materials effectively inhibit spoilage and pathogenic microorganism growth on food surfaces [1,31].

The study involved the preparation of C-1, C-2, and C-3 nanoemulsions by blending thyme, cardamom, and clove essential oils with carboxymethyl cellulose (CMC). Optimized levels were determined using different concentrations, and their application was then compared to kiwifruit sample results. The potential of these nanoemulsions has indicated their effective results against bacteria and fungi. The current research is innovative in that the combination of different essential oils (cardamom, thyme, and clove) with different proportions of CMC and glycerol levels nano-emulsions were prepared for coatings of kiwifruits. Furthermore, the research emphasized their industrial application to the fruit and vegetable industry. The study highlights a notable transition towards exploring natural ways for fruit preservation, which has the potential to open up new avenues for innovative techniques in food preservation.

## 2. Materials and method

### 2.1. Chemicals

Carboxymethyl cellulose (CMC) was purchased from Merck (Molsheim, France), and the essential oils of cardamom, clove, and thyme and tween 80 were purchased from Sigma-Aldrich (United States). A selection of ripe, unblemished, and robust mature light red kiwifruits was purchased randomly from local marketplaces in Faisalabad, Punjab,

Pakistan.

### 2.2. Preparation of nanoemulsion

The nanoemulsion was prepared according to the previously described method by Das et al. [15], with some modifications. Several concentrations of CMC: T-80 and T-80: EOs have been prepared and tested (1,1, 2:1, 1:2, 1:3, and 1:5). The coating that consisted of a 1:1 ratio of CMC: T-80 and T-80: EOs exhibited the highest stability among all the coatings tested. Consequently, this coating was employed in processing all other coating preparations. For solution preparation, a 1 % CMC solution is first prepared with ultrapure water (Milli-Q water purification system, Merck, Molsheim, France). Briefly, 10 g of CMC is dissolved in 1 l of water at 90 °C for 1 h with continuous magnetic stirring at 1200 rpm to dissolve all lumps of CMC in the water and obtain a homogeneous solution. The solution is then homogenized for 15 min using a high-pressure homogenizer (T25 digital Ultra-Turrax, IKA, Staufen, Germany). At 35 °C, 10 mL of tween-80 surfactant is added to the CMC solution while stirring at 1500 rpm using a magnetic stirrer. The oil combinations were mixed into the solution in the last phase to prepare a coarse emulsion. The emulsion is then sonicated for 1 h in an ultrasonication probe machine (VCX 500, Vibra-Cell, Newtown, CT, USA) to prepare an oil-embedded nanoemulsion. For multiphase essential oils, add equal amounts of each essential oil to a 50-ml beaker and then transfer 10 ml of the mixture to the solution to prepare a nanoemulsion. Table 1 provides the various combinations of essential oils and other components utilized in formulating C-1, C-2, and C-3 nano-emulsions.

### 2.3. Sample collection

Kiwifruit that had reached optimal ripeness and were in good condition were obtained from local marketplaces in the Faisalabad region. Several considerations, such as obtaining disease-free plant specimens, are considered when collecting samples. Selected specimens determined to be in good condition and of high worth were gathered and then placed in a refrigerator for a brief duration in anticipation of further processing.

### 2.4. Coating application

The kiwi fruits were taken from a refrigerated storage facility, and the collected kiwifruit samples underwent a sterilization procedure by washing them with a sodium hypochlorite solution with a concentration of 100 ppm. The fruits were flushed with tap water and left to drain for 7 min. The fruits that had been washed were subsequently placed in storage for additional processing. Subsequently, the kiwifruit sample was immersed in three different coating formulations: C-1 (containing 1 % carboxymethyl cellulose (CMC) combined with thyme and cardamom essential oils (EOs)), C-2 (consisting of 1.25 % CMC mixed with thyme and clove EO), and C-3 (containing 1.5 % CMC infused with clove, thyme, and cardamom EO), for 3 min. Simultaneously, the kiwi specimens submerged in water were assigned as the control group. The coatings underwent drying at room temperature, precisely at 15 ± 2.0 °C, and were then kept in polypropylene trays measuring 14 × 9 × 7

**Table 1**

Optimized nano-emulsions concentrations of C-1, C-2, and C-3 used for the coating of kiwifruit samples.

Nanoemulsion name	CMC concentration	EOs concentration (Thyme: Cardamom: Clove)	Glycerol	Sonication time
C-1	1 %	1:1:0	1 %	120 min
C-2	1.25 %	1:0:1	1 %	120 min
C-3	1.5 %	1:1:1	1 %	120 min

cm<sup>3</sup>. Ten kiwi fruit samples were placed in separate trays and stored at 15 ± 2.0 °C for seven days.

## 2.5. Nanoemulsion characterization

### 2.5.1. Particle size, polydispersity index (PDI), and $\zeta$ -potential of coating-forming nanoemulsion

The particle size, polydispersity index (PDI), and zeta-potential were assessed using a particle size and zeta-potential analyzer (Nano-ZS90 model, Malvern Instruments Ltd., UK). To minimize the effects of numerous scattering phenomena, a dilution procedure was conducted on the emulsions with ultra-pure water at a ratio of 1:100. The studies were conducted in triplicate under controlled conditions with a temperature maintained at 25 °C.

### 2.5.2. Fourier transform infrared spectroscopy (FTIR) analysis

Fourier Transform Infrared Spectroscopy (FTIR) was examined using solution samples. Fourier Transform Infrared Spectroscopy (FTIR) was conducted to analyze and identify the functional groups in the nanoemulsion and better understand the structural properties of the nanoemulsion and its components. Additionally, FTIR was used to investigate the interactions and binding affinities between these components. Fourier Transform Infrared (FTIR) spectra were obtained throughout the wave-number range from 4000 to 400 cm<sup>-1</sup> [32].

### 2.5.3. X-ray diffraction (XRD)

An X-ray diffractometer (XRD D8ADVANCE, Bruker, Germany) was used to analyze the X-ray diffraction pattern of carboxymethyl cellulose (CMC) and a lyophilized film of nano-emulsions. The measurements were conducted on a 2 × 2 cm<sup>2</sup> sample. The powder samples were placed within the X-ray diffraction (XRD) specimen holder, with a diameter of 2 cm and a height of 2 mm. The X-ray diffraction (XRD) spectra were obtained using Cu-K $\alpha$  radiation filtered using nickel, resulting in a wavelength ( $\lambda$ ) of 1.54 Å. The scanning rate was adjusted to 0.5° per minute, including a range of 10–70° (20). The experiments were conducted in normal environmental circumstances, using a voltage of 40 kV and a current of 30 mA [33].

### 2.5.4. Determination of morphology of nanoemulsion

The morphology of the lyophilized carboxymethyl cellulose nanoemulsion (CMC-NE) and EOs loaded CMC nanoemulsion (EOs-CMC-NE) was analyzed using the high-resolution scanning electron microscopy (HR-SEM) technique. The analysis was performed using the Evo-18 researcher instrument (Zeiss, Germany). The instrument was operated at an accelerating voltage of 15 kV. To improve the electrical conductivity, a coating of gold was applied to the samples using the Nova NanoSEM 250 sputter coater (Quorum, Q150R-ES, Lewes, UK) prior to analysis [33].

### 2.5.5. Antibacterial and antifungal activities

The antibacterial and antifungal activity of the nanoemulsion was examined using the agar disc diffusion method, as outlined by Du et al. [34]. This work focused on *Staphylococcus aureus* and *Escherichia coli*, which are examples of Gram-positive and Gram-negative bacteria, respectively. Furthermore, an assessment was conducted to determine their antifungal efficacy against *Aspergillus niger* and *Aspergillus flavus*. The test strains were subjected to an overnight culture in nutrient media. The subsequent procedure involved the preparation of bacterial and fungal suspensions. The procedure involved mixing 0.3 mL of the overnight culture with 8 mL of a saline solution containing 0.85 % NaCl, which adhered to the 0.5 McFarland standards. Then, 0.2 mL of the prepared suspension was uniformly dispersed on solidified Mueller Hinton agar (MHA) in Petri dishes using a spreader. The nanoemulsion was used to coat circular discs measuring 1.7 cm in diameter. The discs were sterilized by UV radiation for 15 min in a laminar airflow environment.

## 2.6. Qualitative attributes

### 2.6.1. Percentage weight loss ratio

The weight loss of kiwifruit was quantified using the methodology outlined by Nian et al. [35]. Determining the % weight reduction relative to the initial weight required measuring samples at both the beginning (0 days) and the conclusion of each storage period. To compute the total % weight loss, subtract the final weight of the sample from the initial weight. The data was given as the percentage reduction in the initial weight. The analysis was performed on three separate occasions.

$$\text{Weight Loss (\%)} = \frac{\text{initial weight} - \text{final weight}}{\text{initial weight}} \times 100 \quad (1)$$

### 2.6.2. Decay incidence

The occurrence of kiwifruit decay was assessed using the methodology outlined by Xu et al. [1]. The percentage degradation of the kiwi samples was evaluated by examining the occurrence of rotting on their surface at the beginning and conclusion of each storage period. Each treatment was replicated three times. During the analysis, samples underwent visual examination to detect spoiling indications, such as hue alterations, evident structural impairment, and overall aspect. When about 70 % of the fruit surface area exhibited degradation, those samples were excluded from the analysis. The decay percentage was determined by dividing the decaying samples by the initial number of samples and multiplying the result by 100.

$$\text{Decay Incidence (\%)} = \frac{\text{Decay Sample}}{\text{Initial number of samples}} \times 100 \quad (2)$$

### 2.6.3. Total suspended solids and titratable acidity

The total suspended solid content in kiwifruit was determined using the methodology outlined by Xu et al. [1]. The juice from kiwi slices was extracted using a juice mixer grinder produced by National Enterprises in Karachi, Pakistan. The obtained juice was combined and passed through a Whatman filter paper No. 2 for filtration. The juice's total soluble solids (TSS) were quantified using an Atago Co. hand refractometer in Tokyo, Japan. The TSS analysis was performed thrice to ensure precision, and the outcomes were reported as percentages.

The titratable acidity was determined via the titration methodology outlined by Nian et al. [35]. A ten-gram suspension of ground kiwi samples was combined with 100 mL of distilled water. The suspension was further filtered using a Whatman No. 2 filter paper. A titration was conducted on the filtrate, which had a volume of 10 mL. A solution of NaOH with a concentration of 0.1 mol/L was utilized, and the pH at which the reaction reached its endpoint was determined to be 8.0. An indicator, phenolphthalein, was employed at a concentration of 0.1 g/100 mL.

### 2.6.4. Maturity index

The maturity index of a commodity is a quantitative measure used to evaluate the degree of ripeness or decay of a certain fruit commodity. The ratio (TSS/TA), utilized for assessing the quality of fruits and vegetables [36], was calculated by dividing the Total Soluble Solids (SS) value by the Titratable Acidity (TA) value. The TA index varies following the maturation of fruits and vegetables, as it decreases during the ripening process [37].

$$\text{Maturity Index} = \frac{\text{Total Soluble Solids (TSS)}}{\text{Titratable Acidity (TA)}} \quad (3)$$

### 2.6.5. Ethylene production

The ethylene production and respiration rate assessment were performed following the technique described by [1], with minor modifications included in the experimental protocol. In this experiment, kiwifruit samples were placed inside a container that was well sealed, ensuring no exchange of air, with a total capacity of 9.7 l on the first day.

During the experiment, a syringe collected gas samples from the headspace on specific days (1, 5, 10, 15, 20, 25, and 30). These samples were then analyzed using a gas chromatograph (FuliGC9790II, Zhejiang, China) with an FID detector and a GDX-502 stainless column (3.0 m × 3.0 mm). The amount of ethylene released was determined by calculating the peak area of the ethylene standard, which allowed for the quantification of ethylene production. Helium was used as the carrier gas, and the column temperature was maintained at 70 °C. In contrast, the detector was kept at 150 °C while the injection port temperature was adjusted to 100 °C. The results are shown in units of micrograms per gram per hour ( $\mu\text{g/g/h}$ ).

#### 2.6.6. Firmness determination

The firmness of the kiwifruits was assessed using the TA-TX plus texture analyzer manufactured by Stable Micro System Ltd. in the United Kingdom. This method was previously described by Yun et al. [38]. The experiment involved performing a puncture test using a cylindrical probe with a diameter of 3.5 mm. The probe was driven into the material at a constant speed of 10 mm/s, resulting in a penetration depth of 10 mm. Three fruits were selected randomly from each treatment, and the firmness of each fruit was measured on both sides of the equatorial zone. The outcomes were quantified in units of kilograms per square centimeter ( $\text{kg.cm}^{-2}$ ).

#### 2.6.7. Microbiological analysis

The kiwifruit was subjected to a microbiological analysis using the approach developed by Rojas-Graü et al. [39]. The sample (25 g) was combined with 225 mL of sterile physiological saline solution, which has a concentration of 8.5 g per 1000 mL. The mixture was homogenized in a clean environment using a VOSHIN-600R homogenizer produced by Wuxi Voshin Instruments, LTD in China. The sample (1 ml) from each sample was transferred to plates containing plate count agar to determine the total aerobic counts and rose Bengal agar to determine the presence of mold and yeast. Each treatment underwent serial 10-fold dilutions. Afterward, the plates designed for measuring the total number of aerobic microorganisms were placed in an incubator set at 37 °C for 48 h. In contrast, the plates specifically used to evaluate the growth of fungus and yeast were kept in an incubator at a temperature of 28 °C for 3 days. Two duplicates were performed, and the findings were expressed as logarithmic colony-forming units per gram ( $\log \text{CFU/g}$ ).

#### 2.6.8. Sensory evaluation

The sensory evaluation of kiwifruits, including both treated and control samples, was performed using the hedonic scale methodology described by Escribano et al. [40], with certain adjustments. During the duration of storage, a panel of 15 judges with modest expertise evaluated the characteristics of color, texture, smell, taste, and overall acceptability on days 1, 5, 10, 20, 25, and 30. The researchers employed a ten-point descriptive hedonic scale to assess the overall evaluation of the sample, with a rating of 10 denoting a pronounced positive attitude and a rating of 1 denoting a pronounced negative feeling. The threshold for acceptability was established as anything below 5.5.

#### 2.7. Statistical analysis

Each experiment was conducted with three technical replicates. The data was analyzed using a one-way analysis of variance. The statistical software OriginPro was used to analyze variance (ANOVA). The post hoc Tukey Honest test was used to compare the mean values across various storage durations. Significant statistical differences were discovered when the  $p$ -value was  $<0.05$  ( $p < 0.05$ ).

### 3. Results and discussion

#### 3.1. Particle size, polydispersity index (PDI), and $\zeta$ -potential of coating-forming nanoemulsion

The nano-size and  $\zeta$ -potential of edible nanoemulsion coatings prepared with carboxymethyl cellulose and Essential Oils were analyzed (Fig. 1a). The research compared nanoemulsions at different ultrasonication times (10, 20, 30, 60, and 120 min) to determine how ultrasonication affects their size and  $\zeta$ -potential.

The ultrasonic emulsification process resulted in nano-emulsions (C-1, C-2, and C-3) with droplet sizes of  $81.3 \pm 2.3$  nm,  $115.3 \pm 4.2$  nm, and  $63.2 \pm 3.2$  nm, respectively. Notably, ultrasonic treatment's high energy sheer force played a pivotal role in generating these nano-sized emulsions (C-1, C-2, and C-3). The findings strongly affirm that extending the ultrasonication duration leads to a systematic reduction in droplet sizes. This observation aligns with the proposition that prolonged exposure to high-energy sound waves has the potential to generate progressively smaller nano-droplets, as evidenced by the study conducted by [15]. DLS showed that almost all nanoemulsion intensity peaks are narrow and monomodal. This suggests that nanoemulsions were evenly distributed [15]. The low PDI range ( $0.216 \pm 0.01$  to  $0.141 \pm 0.07$ ) for all nanoemulsions approved this conclusion. PDI values for C-1, C-2, and C-3 nano-emulsions were  $0.133 \pm 0.01$ ,  $0.144 \pm 0.03$ , and  $0.121 \pm 0.01$ . Tween 80 made nanoemulsions due to its hydrophilic-lipophilic balance (HLB = 15). Tween 80, a small-molecule surfactant, absorbed droplets better than polymer-based surfactants [41,42]. Ultrasonication may boost adsorption. This quick absorption reduces droplet size and avoids re-coalescence.

The Zeta Sizer analysis of three nanoemulsions, characterized at time intervals of 10, 20, 30, 60, and 120, is shown in Fig. 1b. A key factor in determining emulsion stability was the  $\zeta$ -potential. The investigation revealed that the nanoemulsions C-1, C-2, and C-3 droplets had negative  $\zeta$ -potential values of  $-50.4$ ,  $-108$ , and  $-89.2$  at maximum ultrasonication time. According to Yin et al. [43], a  $\zeta$ -potential value above  $+30$  mV or falling below  $-30$  mV indicates a significant level of electrostatic repulsion between droplets, impeding the flocculation process. A negative  $\zeta$ -potential in the millivolts range signifies the consistent production of nanoemulsions. The carboxylate group in the solution form of carboxymethylcellulose is responsible for the negative zeta potential of all CMC-based nanoemulsions, which can be shown in the FTIR spectrum of CMC nanoemulsions. Arancibia et al. [44] discovered that our findings align with theirs, indicating that the addition of CMC to the nanoemulsion did not have a significant impact ( $p > 0.05$ ) on the zeta size. This is because the average particle size, as measured by zeta, only showed slight variations across samples with different oil contents.

However, adding CMC considerably raised zeta potential results for both oil concentrations, contradicting current research. The CMC-CEONE had a pH of  $7.3 \pm 0.48$ . This neutral pH prevents food from being tested again.

#### 3.2. Fourier transform infrared spectroscopy (FTIR) interaction studies

The FTIR spectra of carboxymethyl cellulose, tween-80, glycerol, C-1, C-2, and C-3 coatings are analyzed and shown in Fig. 2a. In carboxymethyl cellulose (CMC), bands at  $3300$  and  $3400 \text{ cm}^{-1}$  correspond to hydroxyl (OH) group stretching vibrations, hydrogen bonding, and free hydroxyl groups in cellulose. The  $2900$ – $3000 \text{ cm}^{-1}$  wavelength bands are linked to C—H bond stretching vibrations in methylene and methyl groups [45]. The strong band peak at  $1640 \text{ cm}^{-1}$  may be caused by carboxylate groups, which differ from carbonyl (C=O) group stretching vibrations in CMC. C=O stretching vibrations from carboxylate groups produced during carboxymethylation produce a peak of about  $1600$ – $1650 \text{ cm}^{-1}$  [45,46]. The  $800$ – $1100 \text{ cm}^{-1}$  bands are C—C and C—O—C stretching vibrations.

This vibration is typical of cellulose backbone structure. Peaks

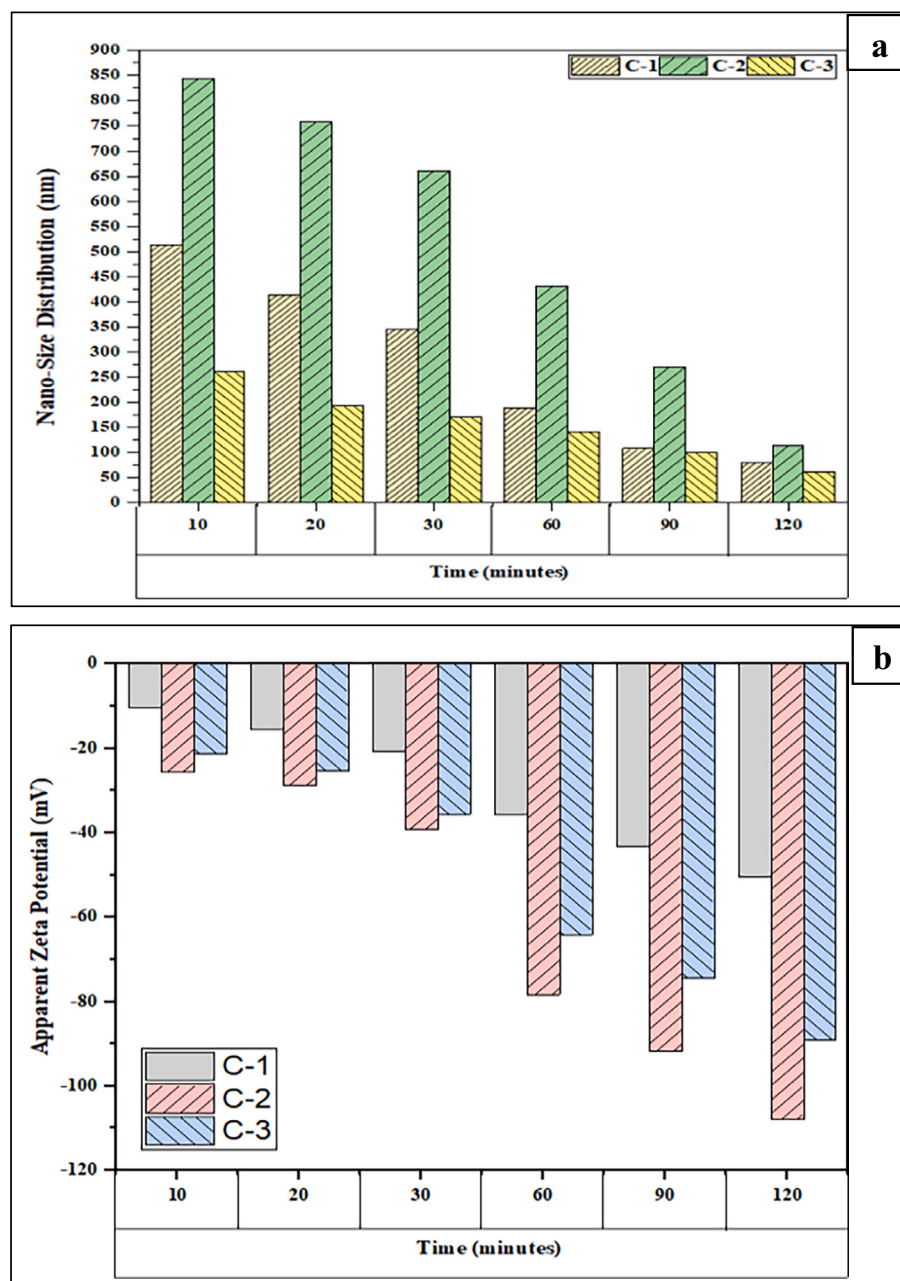


**Fig. 1.** Nanosized distribution of the prepared nano emulsions (C-1, C-2, and C-3) at various time intervals after the sonication (a); Zeta potential values of the prepared nano emulsions (C-1, C-2, and C-3) at various time intervals after the sonication (b).

between 1000 and 1300 cm<sup>-1</sup> suggest molecular C—O bond stretching vibrations. Due to C—O bonds like ether (C-O-C) connections, this area sometimes has numerous peaks [47,48]. Hydroxyl (OH) group stretching vibrations in Tween-80 cause a peak at 3450 cm<sup>-1</sup>, showing hydrogen bonding and free hydroxyl groups. Peaks at 2900–3000 cm<sup>-1</sup> show C—H bond stretching vibrations in the molecule's alkyl chains [49]. A prominent peak about 1700–1750 cm<sup>-1</sup> reflects carbonyl (C=O) group stretching vibrations observed in ester functionalities. C—C and C-O-C stretching vibrations are represented by 800–1100 cm<sup>-1</sup> bands, like CMC [50]. These vibrations correspond to Tween-80's hydrocarbon chains and ether bonds. Tween-80's ethylene oxide units may have distinctive peaks at 1100–1300 cm<sup>-1</sup> [51]. The large peak between 3200 and 3500 cm<sup>-1</sup> in glycerol, a typical plasticizer, indicates hydroxyl (OH) groups. The stretching vibrations of hydrogen-bonded OH groups cause this peak. Peaks at 2900–3000 cm<sup>-1</sup> suggest C—H bond stretching vibrations in glycerol alkyl chains [52]. Peaks at 1000–1300 cm<sup>-1</sup> suggest

glycerol C—O bond stretching vibrations. These vibrations are typical of alcohol (OH) groups. Bending vibrations of C-O-H groups peak around 1600–1650 cm<sup>-1</sup> [53]. Hydroxyl group configuration affects this peak. 1350–1450 cm<sup>-1</sup>, C—H bond bending vibrations occur in the molecule [54]. For the C-1 nanoemulsion solution, a distinctive new peak in this region was assigned to C—O stretching vibrations. It might relate to specific C—O bonds within the components present in the nanoemulsion, such as those from CMC or ester linkages in Tween-80. The C-1 nanoemulsion pattern shows CMC characteristic peaks and additional peaks (930–1090 cm<sup>-1</sup>), possibly attributed to C—O bonds in components like CMC or ester linkages in Tween-80. The carbonyl group in the CMC exhibits C=O stretching vibration in the 1600–1650 cm<sup>-1</sup> wavelength region. The interaction between Tween-80 and CMC and the hydrogen bond between their proton donor groups (—OH) and proton acceptor groups (C=O) may be indicated by the intense peak and shift in absorption spectra at around 1650 cm<sup>-1</sup>. The peak at 3000 cm<sup>-1</sup> and

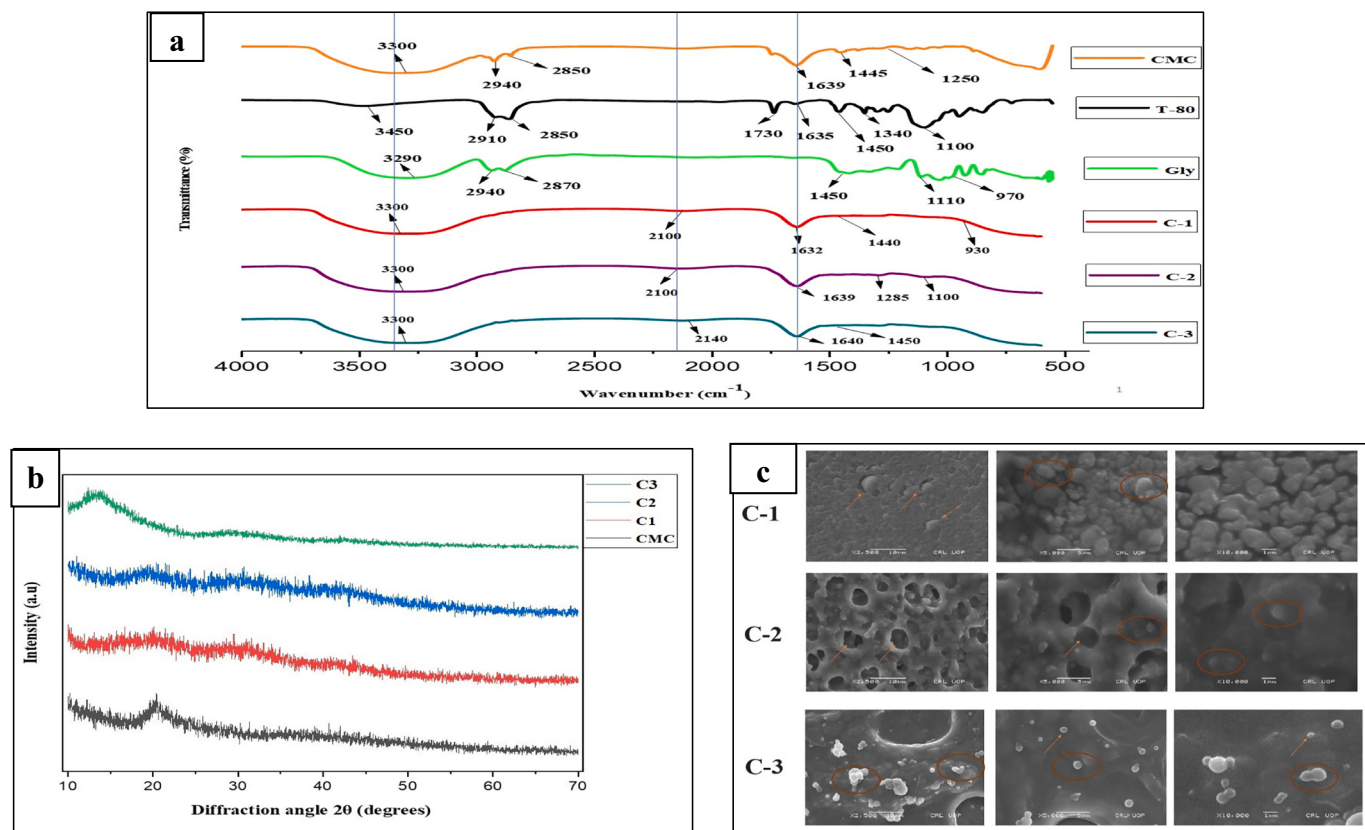


**Fig. 2.** FTIR spectrums of nanoemulsion components, carboxymethylcellulose, T-80, glycerol, and prepared nanoemulsion (C-1, C-2, and C-3) (a); XRD spectrum of Carboxymethyl cellulose (CMC) and prepared nanoemulsions C-1, C-2, and C-3 (b); Scanning electron microscopy (SEM) at various resolutions for the prepared nanoemulsions of lyophilized films (C-1, C-2, and C-3) (c).

wide peak at  $3300 \text{ cm}^{-1}$  correspond to C—H and —OH stretching vibrations, respectively. These two peaks have moved in wavelength and intensity compared to pure T-80 and CMC, proving their immiscibility and connection. Adding clove EO to C-2 nanoemulsion solutions changes the intensity of the wavelength range  $3300\text{--}3500 \text{ cm}^{-1}$ , particularly the peak at  $3300 \text{ cm}^{-1}$ , which is attributed to the O—H stretching vibration in the C-2 nanoemulsion. The  $3400$ ,  $2900$ , and  $1650 \text{ cm}^{-1}$  shifts in C-2 nanoemulsion, representing O—H, C—H, and C=O stretching, respectively, indicate changes in vibration modes and intensities due to extensive intermolecular interactions. Notably influenced by varying essential oil ratios, diverse functional groups contribute to these shifts. In C-3 Nanoemulsion, characteristic shifts occur at  $1660\text{--}1640 \text{ cm}^{-1}$  and  $3450\text{--}3550 \text{ cm}^{-1}$ , including C=O and O—H stretching peaks at  $1654$  and  $3506 \text{ cm}^{-1}$ . Crucially, peaks at  $1654 \text{ cm}^{-1}$  and  $3400 \text{ cm}^{-1}$  shift to lower and higher wavelengths, respectively, compared to C-2 nanoemulsion, highlighting dynamic intermolecular interactions. Considering different essential oil ratios, this analysis comprehensively explains observed infrared spectra shifts.

### 3.3. XRD crystallography study

X-ray diffraction (XRD) assessed the crystalline and non-crystalline features of the C-1, C-2, and C-3 nano-emulsions. Fig. 2b illustrates the XRD analysis of CMC, C-1, C-2, and C-3 nanoemulsions. The crystalline structure of carboxymethylcellulose (CMC) exhibits sharp peaks at  $2\theta = 22^\circ$ , indicating its crystalline behavior [47,55]. Specifically, the XRD pattern of CMC reveals distinct peaks at  $21.24^\circ$  and  $38.74^\circ$ , highlighting its crystalline nature. Moving to the nanoemulsions, the XRD pattern of C-1 demonstrates a shift in major peaks of crystallinity. Major intensity peaks at  $2\theta = 20.31^\circ$ ,  $20.10^\circ$  &  $17.0^\circ$  also observed.

For instance, the peak at  $2\theta = 38.74^\circ$  shifts to a lower peak at  $2\theta =$

$33^\circ$  and diminishes in apparent intensity. In contrast, C-3 nanoemulsion exhibits a unique XRD pattern with crystalline and non-crystalline regions. Notably, the C-3 film displays a strong intensity peak at around  $2\theta = 15.23^\circ$  and a negligible peak at  $2\theta = 32.11^\circ$ , indicating heightened crystallinity compared to C-1 and C-2 films. The increased essential oil concentrations and elevated carboxymethyl cellulose (CMC) content from 1 % to 1.25 % contribute to this enhanced crystallinity in C-3. Meanwhile, C-1 is characterized by specific liquid entities such as T-80, essential oils, and water molecules. At the same time, C-2 exhibits a lyophilized film pattern marked by two peaks at  $2\theta = 22.35^\circ$  and  $35.57^\circ$ , indicative of lower crystallinity attributed to favorable miscibility between T-80, essential oils, and CMC. Additionally, the XRD pattern of C-2 shows narrower and less intense peaks than C-1. The lower crystallinity observed in C-2 aligns with the successful synthesis of C-2 nanoemulsions, further emphasized by noticeable changes induced by T-80 essential oils in the XRD pattern's lower intensities, resembling characteristics similar to C-1 [15].

### 3.4. Morphology study by scanning electron microscopy

The confirmation of the particle size distribution of the nanoemulsion was achieved using scanning electron microscopy (SEM) analysis. The scanning electron microscopy (SEM) images shown in the current study (Fig. 2c) depict the presence of spherical droplets inside an edible coating dispersion, whereby smooth oil globules are uniformly dispersed.

The C-3 nanoemulsions had a homogeneous distribution and absence of observable pores, indicating a non-porous structure. This may be due to the excessive crystallinity or aggregation of the nanoemulsion. A higher concentration of carboxymethylcellulose in C-3 could contribute to reduced flexibility and a more rigid appearance. In contrast, C-2

displayed visible voids, pores, or irregularities, indicating the presence of empty spaces within the film. The surface texture of C-2 appeared rigid or stiff, potentially with sharp edges, and showed no deformation under microscopic examination. C-1 film exhibits surfaces with uniformly distributed, spherical, or rounded globules that lack distinct spaces or voids. Globules may exhibit proximity or contact with one another, resulting in a cohesive surface appearance. The particle sizes for C-1, C-2, and C-3 were determined to be  $91 \pm 3.6$  nm,  $100.41 \pm 4.2$  nm, and  $71.39 \pm 5.6$  nm, respectively, consistent with the findings of our dynamic light scattering (DLS) study. Previous research has shown that CMC can produce distinct globule-shaped homogeneous nano-emulsions and nano drops evenly distributed throughout the structure. Prior studies have examined the development of nano-emulsions using carboxymethyl cellulose (CMC) as a primary ingredient and cardamom essential oils (EOs) as an antibacterial agent. The nano-emulsions exhibited a uniform distribution of essential oils across the nano-emulsion framework [15]. Similarly, another nano emulsion sample containing beta-carotene displayed spherical nano drops identified as having a smooth surface using scanning electron microscopy (SEM) [56].

### 3.5. Antibacterial and antifungal activities (zone of inhibition)

The evaluation of nano-emulsions, namely C-1, C-2, and C-3, against bacterial and fungal strains revealed notable variations in antimicrobial activity. C-3, composed of clove, thyme, and cardamom essential oils, exhibited the highest inhibition against both *Escherichia coli* (*E. coli*) and *Staphylococcus aureus* (*S. aureus*), with bactericidal zones measuring 14.13 mm and 12.39 mm, respectively. In contrast, C-1, comprising thyme and cardamom essential oils, displayed lower effectiveness with inhibition zones measuring 10.45 mm and 9.46 mm for *E. coli* and *S. aureus*, respectively.

Similar trends were observed in antifungal activity against *Aspergillus niger* and *Aspergillus flavus*. The coating C-3 demonstrated the highest

antifungal activity, with inhibition zones measuring 14.78 mm and 16.68 mm, while C-1 exhibited smaller zones measuring 10.45 mm and 12.67 mm. The variation in antimicrobial efficacy can be attributed to each formulation's specific composition of essential oils. Essential oils, such as those found in thyme, cardamom, and clove, contain bioactive compounds that disrupt fungal cell membranes, impede enzymatic activities, and inhibit fungal development. The synergistic effect of combining these essential oils in C-1 may contribute to its extensive antibacterial and antifungal activity.

Furthermore, differences in formulation, including variations in essential oil quantities and their synergistic interactions with carrier components like CMC and Tween-80, can influence the overall antimicrobial properties. These factors play a crucial role in determining the effectiveness of nano-emulsion coatings against a spectrum of microbial diseases. The observed variations in antibacterial and antifungal activity among C-1, C-2, and C-3 nano-emulsions highlight the importance of understanding the specific interactions and synergies between essential oils and formulation components. Tailoring formulations based on such considerations can lead to the development of versatile antimicrobial coatings with enhanced efficacy for diverse applications.

### 3.6. Visual appearance, percentage weight loss, and decay incidence

The visual appearance of control and coated samples are recorded and presented in Fig. 3a. The weight loss percentage of kiwifruit samples is shown in Fig. 3b. The results show that upon harvest, a consistent increase in weight loss has been documented throughout the storage period under controlled conditions of  $10 \pm 2$  °C temperature and 90–95 % relative humidity. The combined treatment of C-3 NM showed a remarkable impact on reducing weight loss in kiwifruit. On the 30th day of the duration, kiwifruit treated with C-3 nano-emulsion experienced only a 15.26 % total weight loss in treated samples, significantly compared to control samples. This significant inhibitory effect ( $p < 0.05$ ) on weight reduction in kiwifruit was evident in the investigation, as

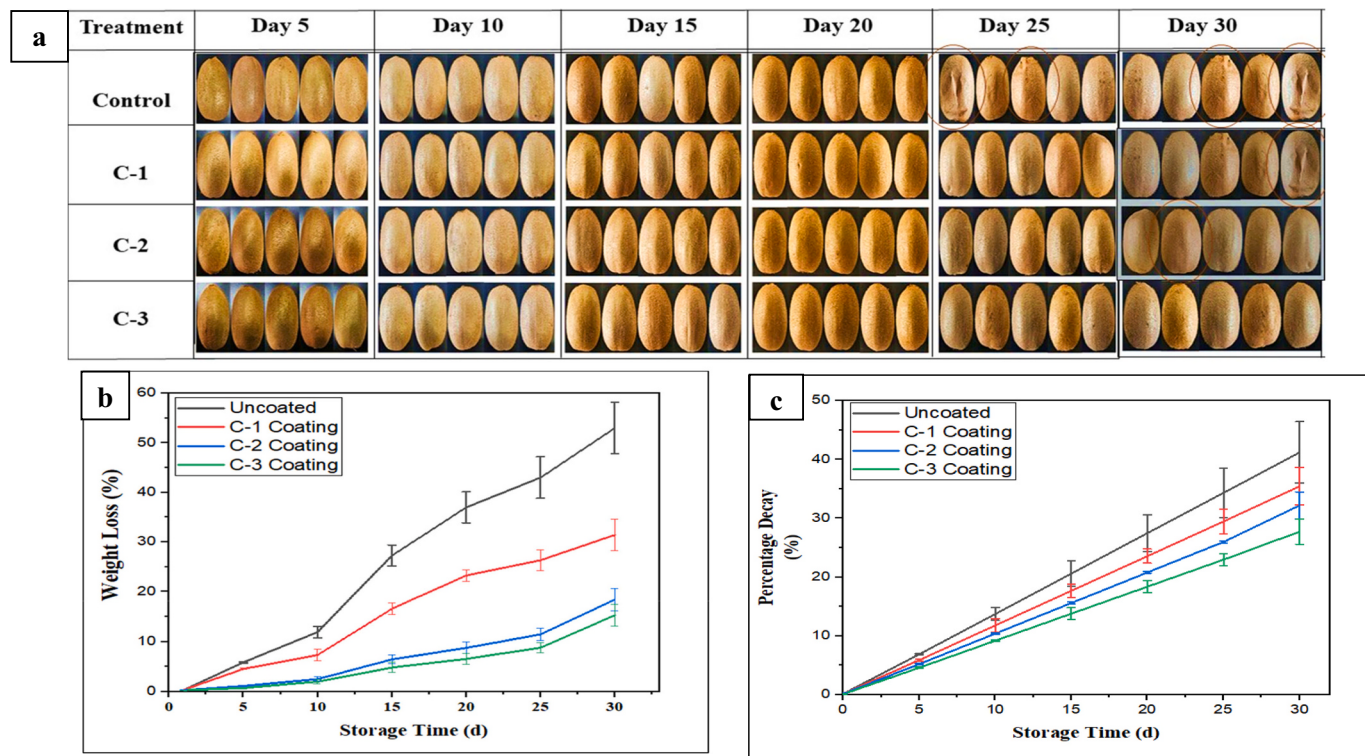


Fig. 3. Visual appearance of kiwifruit during the shelf life of control samples and kiwifruit treated with nanoemulsions (C-1, C-2, and C-3) (a); Weight loss (%) comparison of control kiwifruit samples and coated kiwifruit samples (b); Decay (%) comparison of control kiwifruit samples and coated kiwifruit samples (c).

illustrated in the graphical representation of Fig. 3b. Moving to the treatment involving C-2 NM, it demonstrated a superior reduction rate in weight loss compared to C-1 NM. Specifically, C-2 nano-emulsion showed a higher reduction rate of 65.30 %, while C-1 NM exhibited a 40 % reduction rate compared to the control. The results clearly emphasized the notable advantage of C-2 NM treatment over C-1 NM in inhibiting weight loss in kiwifruit, with statistical significance ( $p < 0.05$ ) evident in Fig. 6. Regarding C-1 NM, it also exhibited a reduction effect on weight loss in kiwifruit. However, compared to C-2 NM, its reduction rate was lower at 31.43 %. This indicates that while C-1 NM contributed positively to inhibiting weight loss, its efficacy was surpassed by the superior performance of C-2 NM.

The study by Das et al. [15] revealed promising outcomes regarding using nanoemulsion edible coatings on harvested kiwifruit. Their formulated nanoemulsion, comprising carboxymethyl cellulose (CMC) and cardamom essential oil, effectively decreased decay incidence and weight loss in the fruit. Similar positive effects were observed previously in tomatoes, where these coatings significantly minimized weight loss compared to uncoated tomatoes following a 15-day storage period. Manzoor et al. [57] studied the effects of varying CMC concentrations and alginate-based coatings on fruit weight loss during storage, which causes shriveling and degradation. The lowest weight loss in kiwi slices during storage was 8.0 % with nanoemulsion coating C-3. Different vanillin concentrations did not affect weight loss. Emulsion coatings produce a thick covering on fruit surfaces to prevent water and weight loss. Fig. 3c demonstrates the significant impact of visual appearance on the decay rate. The decay percentage showed a progressive rise in the decay occurrence of control and nanoemulsions (C-1, C-2, and C-3) treated kiwifruit from day 0 to day 30 of storage.

The C-3 coating had a significant effect in reducing decay when

compared to control samples. The treatment led to a notable 48.68 % reduction in decay rate, which was statistically significant ( $p < 0.05$ ) compared to control kiwifruit. The significant decrease observed in the present investigation was higher than the individual impacts of treatments C-1 and C-2. The decay degree of postharvest fruits is an important external factor for assessing their commercial quality due to their high susceptibility to pathogens [58]. The C-2 coating significantly reduced decay incidence in treated kiwifruits following C-3. The decay occurrence in C-2-treated kiwifruit was 28 % lower compared to control samples. The superior performance C-2 compared to C-1 indicates that combining clove and thyme essential oils in C-2 coatings is crucial. These oils can rapidly disrupt the cell membranes of harmful bacteria, thereby aiding in the mitigation of decay in the treated kiwifruit [59]. The C-1 treatment significantly reduced decay incidence but was less efficacious than the C-2 and C-3 coatings. One possible cause might be the composition of C-1 since it has a lower level of CMC and a more miniature composition of essential oils in the coating. The results have demonstrated that the decay in kiwifruit treated with C-1 was 16.25 % lower compared to control samples on day 30. This outcome indicates moderate effectiveness in reducing decay, although it is not as significant as the impact observed with C-2, particularly C-3 treatments.

### 3.7. Total suspended solids (TSS) and titratable acidity (TA)

The total soluble solid contents of control and nanoemulsion coated (C-1, C-2, and C-3) samples were assessed, and a graphical representation is given in Fig. 4a. In the present experiment, the soluble solid content of the control samples exhibited a gradual increase throughout the storage period. Among the various nanoemulsions studied, C-3 notably affected the soluble solid content of kiwifruit significantly

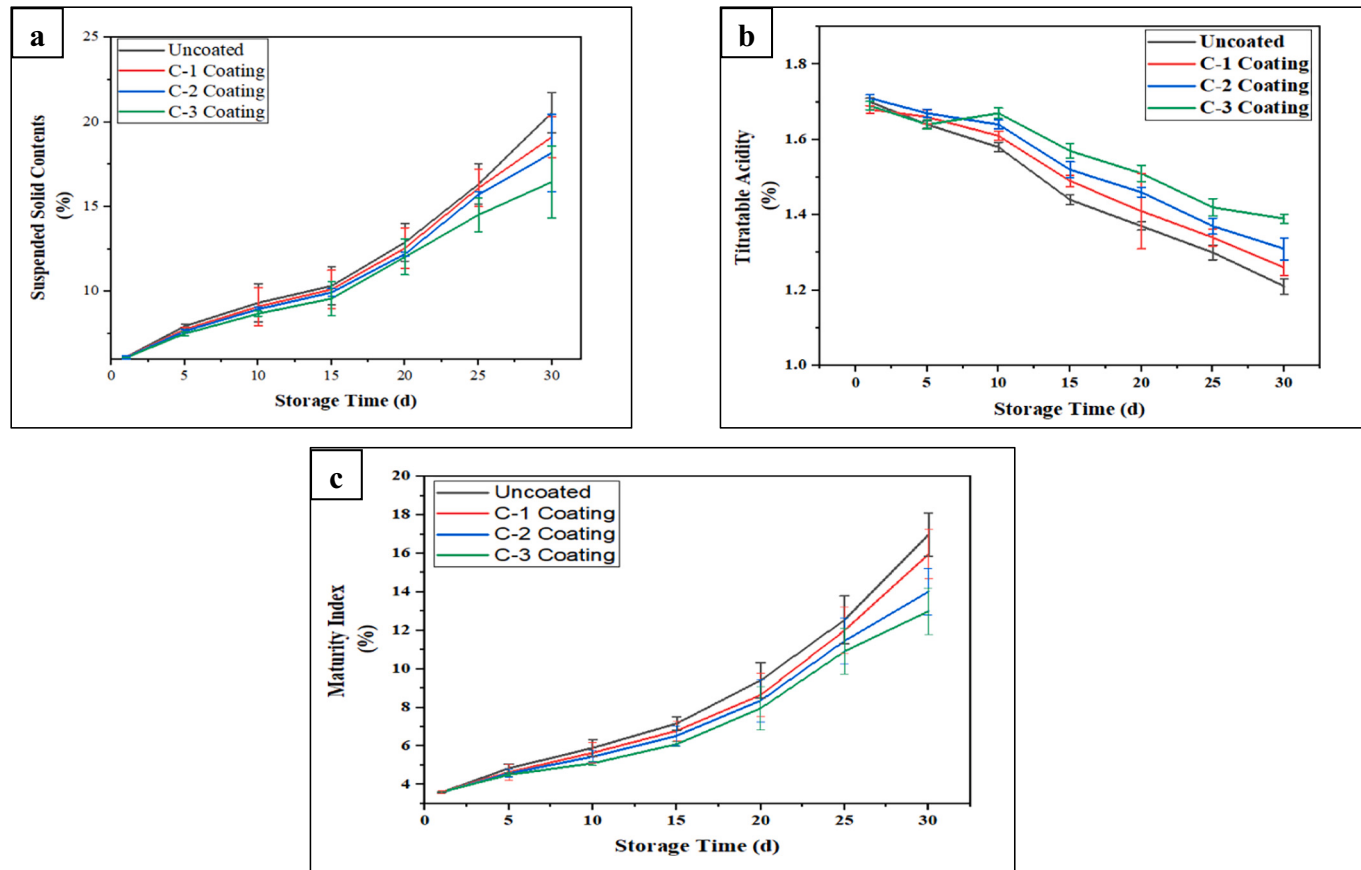


**Fig. 4.** Suspended solid contents (%) comparison of control kiwifruit samples and coated kiwifruit samples (a); Titratable acidity (%) comparison of control kiwifruit samples and coated kiwifruit samples (b); Maturity index (%) comparison of control kiwifruit samples and coated kiwifruit samples (c).

compared to the control samples. From day 10 to day 30 of shelf life, kiwifruit treated with C-3 showed a substantial decrease in soluble solid content, ranging from 6.85 % to 20.00 %. These findings were statistically significant ( $p < 0.05$ ) compared to the control samples. In contrast, the C-2 treatment reduced soluble solid content, notably on the final day of shelf life, with a decrease to 18.18 % (an 11.53 % reduction compared to the control group). However, despite this decrease, statistical analysis using the Tukey test ( $p > 0.05$ ) indicated no significant effect of the C-2 treatment on soluble solid content. Similarly, the C-1 treatment exhibited a decrease in soluble solids, reaching 19.12 % on the last day, showing a 6.95 % reduction compared to the control group. Nonetheless, the Tukey test statistical analysis did not show a significant effect ( $p > 0.05$ ) of the C-1 treatment, similar to C-2, on soluble solid content compared to the control. Similar to our present conclusion, Xu et al. [1] found that control samples gradually increased in soluble solid content to 12.65 % on day 20. On day 20, lysozyme coatings and 1-MCP treatment reduced soluble solids by 11.2 % and 11.9 %, respectively. From day 10 to 20, lysozyme coatings and 1-MCP reduced kiwifruit soluble solid content by 17.2 % to 27.1 %. 1-MCP slowed senescence and enhanced 20 °C kiwifruit preservation.

The sensory effects of titratable acid on kiwifruit after harvest. Control and treated kiwifruit samples showed a similar decline in titratable acid concentration during 30 days of storage (Fig. 4b). Kiwifruit titratable acid content is maintained and improved by coating.

The influence of C-3-treated samples is statistically significant ( $p < 0.05$ ) compared to the control group. The Tukey test showed a substantial change ( $p < 0.05$ ) in titratable acid concentration, notably during later storage phases. The use of C-1 and C-2 coatings delayed the decline in titratable acid concentration, although not significantly ( $p < 0.05$ ). According to the results, this impact was most noticeable in the later storage period. The important relationship between essential oils, carboxymethyl cellulose (CMC) weightage, and kiwifruit titratable acid concentration. The combination affects kiwifruit titratable acid content more than control kiwifruit. Xu et al. [1] used lysozyme-based covering to preserve fresh-cut kiwifruit slices. The research found that storage conditions affected postharvest kiwifruit titratable acid concentration. In particular, lysozyme coatings and 1-MCP therapy improved this. However, 1-MCP therapy was more effective than lysozyme coatings.

### 3.8. Maturity index of fruit samples

The postharvest performance and maturity of kiwifruit are influenced by the ripeness at harvest and the temperature during storage. The kiwifruit samples were evaluated for their maturity index, and the results are shown in Fig. 4c. The maturity index of controlled kiwifruit exhibits a range of approximately 3.60 % to 17 % over 30 days. The application of C-3 coating on kiwifruit demonstrated a noteworthy effect on preserving maturity in comparison to samples that were not treated. During the 30 days, the observed changes in maturity levels for samples treated with C-3 ranged from 3.60 % to 13.0 %. The effectiveness of the C-3 treatment in preventing significant changes in kiwifruit maturity is demonstrated by the maintenance of maturity levels. The effectiveness of the C-2 treatment in preserving the maturity of kiwifruit samples was notable. The observed maturity changes in the C-2-treated samples varied between 3.60 % and 14.02 % during the 30 days. The study results indicate that the C-2 coating effectively prevented significant changes in kiwifruit maturity over the shelf-life period. The C-1 coating demonstrated a significant variation in maturity change among kiwifruit samples, ranging from 3.63 % to 15.90 % over the same duration. The effectiveness of the C-1 treatment in preserving kiwifruit's maturity was lower than the C-2 and C-3 coatings despite its positive impact on inhibiting weight loss and soluble solid content. The variation in maturity level maintenance may significantly impact the assessment of how effective various coatings are in preserving the quality of kiwifruit during storage. The maturity index is a crucial parameter to consider due

to the enduring nature of kiwifruit in the face of environmental stressors [60,61]. This suggests that using essential oils and higher levels of CMC in the C-3 coating improves its barrier properties and antibacterial and antifungal activities. These findings are consistent with the results of our microbiologic analysis.

### 3.9. Ethylene production

The graphical representation in Fig. 5a illustrates the temporal dynamics of ethylene production and respiration rate in the control fruit. It is evident that both variables exhibited a rapid increase, followed by a peak, and subsequently declined to attain their respective maximum thresholds by day 30. Among the various coatings tested, it was observed that C-3 exhibited the ability to significantly delay the initiation of ethylene production and concurrently inhibit the respiration rate of the fruit samples. The observed trend in firmness reduction is consistent with this finding. The results indicate that the ethylene rate increased significantly in fruit treated with C-1 coating compared to other coatings ( $P < 0.05$ ). Furthermore, the ethylene rate reached its highest point on day 15 of the shelf life. Subsequently, there was a gradual decline in the ethylene rate, followed by a final boost on the last day of the shelf life. These findings suggest that C-1 coating has a pronounced impact on ethylene production in treated fruit, with distinct temporal patterns observed throughout the shelf life.

The application of coating C-3 resulted in a decrease in the maximum levels of ethylene production and firmness. Research reveals the peak values of ethylene production in three different coatings, namely C-1, C-2, and C-3. The obtained results revealed that the peak value of ethylene production in C-1 coating was 4.191 µg/g/h, while in C-2 coating, it was 4.019 µg/g/h. Interestingly, the peak value of ethylene production in C-3 coating was significantly lower, measuring only 2.24 µg/g/h ( $P < 0.05$ ). This finding suggests that the ethylene production in C-3 coating is notably reduced compared to the other two coatings. It is noteworthy that the C-3 treated samples, in addition to the other coatings and control samples, did not peak on day 15. The phenomenon of fruit ripening in climacteric species is intricately linked to ethylene production and respiration rate. This process is characterized by the rapid utilization of various metabolic substrates, leading to accelerated maturation and ultimately reducing shelf life [62]. The present study concludes the inhibitory effect of nanoemulsion coatings on ethylene production during room-temperature storage. This finding suggests that such coatings hold promise in terms of retarding the senescence process in freshly harvested kiwifruit [63–65].

### 3.10. Firmness of kiwifruit

The firmness of kiwifruit samples was controlled and treated, which is graphically represented in Fig. 5b. The C-3 nano-emulsified coating showcased a promising capacity to slow down the decrease in firmness in kiwifruit compared to other coatings. While the decrease in firmness was not notably significant, the C-3 coating exhibited a slower rate of firmness reduction, hinting at its potential to delay the ripening process of kiwifruit. This characteristic suggests that, under normal environmental conditions, the C-3 coating might contribute to maintaining a higher level of pulp firmness compared to other coatings, as observed in the study. Moving to the C-2 coating, although specific quantitative data might not have been provided, it can be inferred that it moderately impacted firmness preservation in kiwifruit. However, the details about its comparative effect on firmness reduction are not explicitly stated in the context provided. In contrast, the C-1 coating showed a faster decrease in kiwifruit firmness than other prepared emulsion coatings. This observation implies that the C-1 coating might be less effective in maintaining the firmness of kiwifruit over time when compared to both the C-2 and C-3 coatings.

Furthermore, the evaluation of ethylene production revealed that the C-3 coatings effectively maintained low ethylene concentrations due to

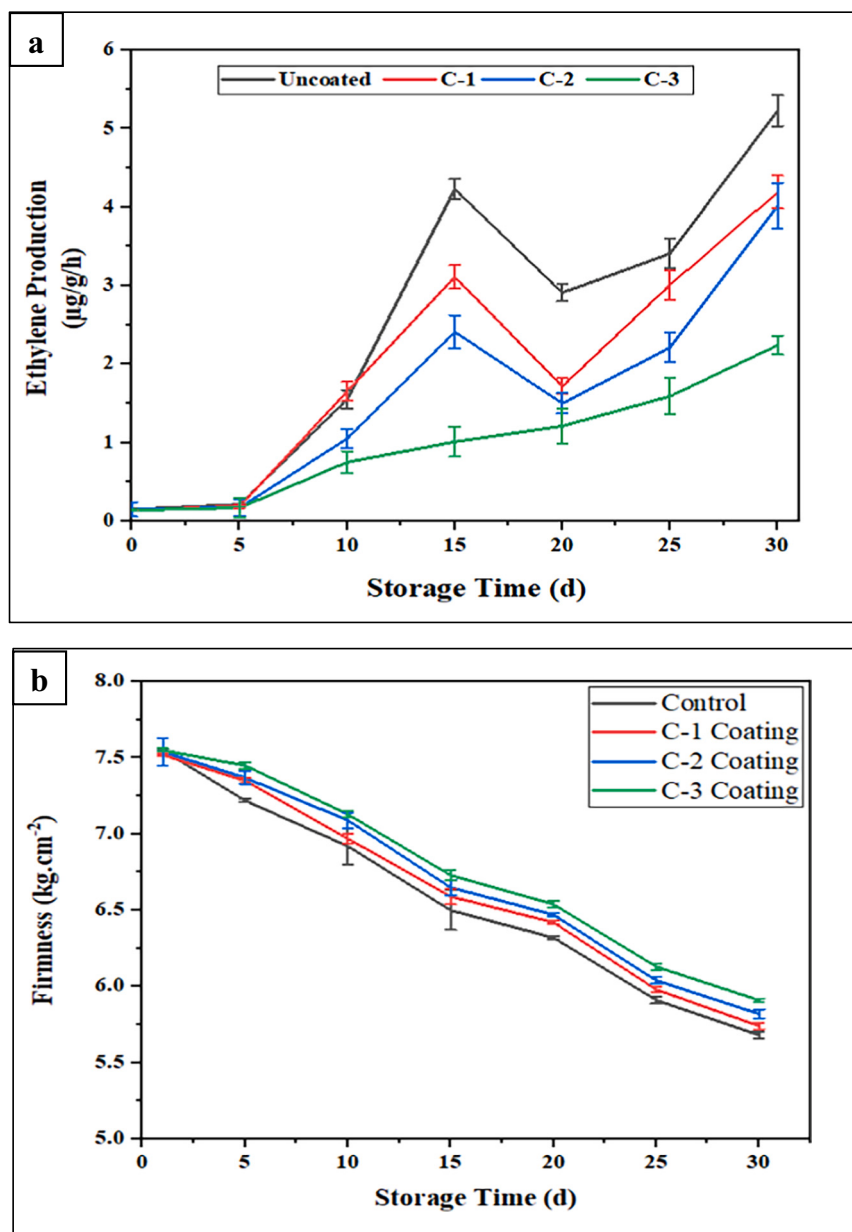


**Fig. 5.** Ethylene production ( $\mu\text{g}/\text{g}/\text{h}$ ) comparison of control kiwifruit samples and coated kiwifruit samples (a); Firmness ( $\text{kg} \cdot \text{cm}^{-2}$ ) comparison of control kiwifruit samples and coated kiwifruit samples (b).

their robust barrier and healing capabilities. This characteristic highlights the potential of C-3 coatings to influence ethylene production in kiwifruit during storage, which plays a crucial role in fruit ripening processes. C-3 coating extends the shelf life of climacteric fruits and vegetables in typical environmental conditions. The decline in kiwifruit firmness after harvest is primarily attributed to several factors: starch hydrolysis of the pulp in the early stage, conversion of pectin to water-soluble pectin in the later stage, liquefaction of cell wall colloid, and eventual destruction of fiber structure. The firmness of fruit samples is strongly correlated with their level of maturity. Fruits, including kiwifruits, undergo a gradual softening and aging process during storage. The firmness change of kiwifruit indicates its maturity and serves as a crucial indicator for assessing its quality [66–68].

### 3.11. Microbiological analysis (bacterial count)

Microbiological analysis, specifically the assessment of the total

bacterial count, is used to determine the extent of bacterial contamination in fruits. The findings of the microbiological analysis can be seen in Fig. 6a, while a graphical representation of the bacterial counts is provided in Fig. 6b. This examination aids in assessing if the fruits comply with the requisite hygienic criteria.

The control samples in our investigation showed a fast rise in the overall bacterial count, reaching a maximum of 18.22 CFU/g on the 30th day of storage. Applying C-1 and C-2 coatings to kiwifruit resulted in a considerable reduction in bacterial growth compared to untreated kiwifruit. The observed impact was ascribed to the bacteriolysis and antibacterial characteristics of the coatings, which were augmented by the inclusion of essential oils in the mixtures. The overall bacterial population in kiwifruit subjected to C-2 treatment exhibited a reduction of 38.36 % on day 30, resulting in a count of 11.23 colony-forming units per gram (CFU/g). However, this impact was not superior to that of C-3. In addition, the C-3 combination treatment demonstrated the most notable impact ( $p < 0.05$ ) on decreasing the overall bacterial population

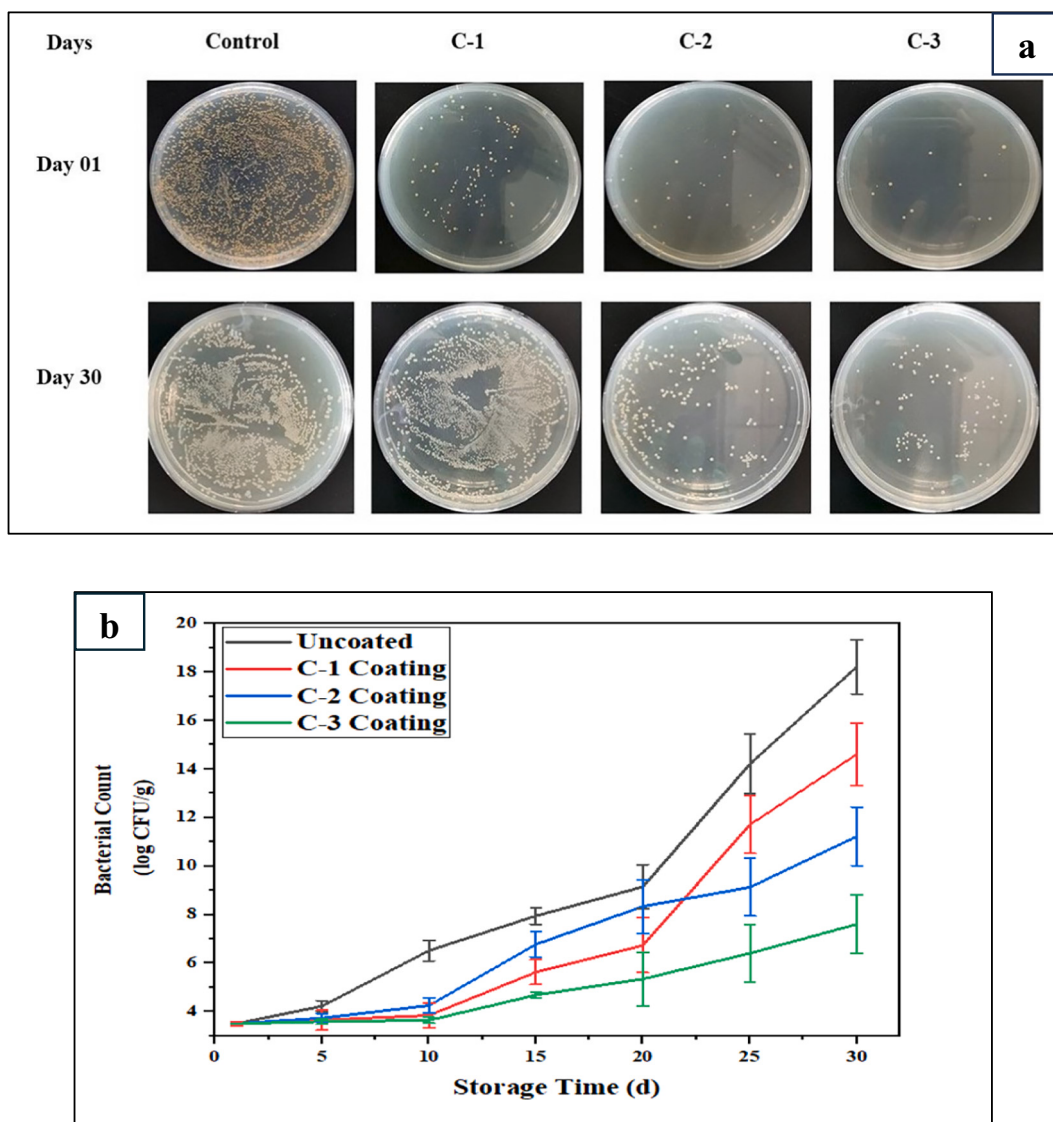


**Fig. 6.** Bacterial counts against microorganisms' comparison of control and nano-emulsions coated kiwifruits (a); Bacterial count (CFU/g) comparison of control kiwifruit samples and coated kiwifruit samples (b).

of kiwifruit. The treatment was reduced by 58.23 % compared to the control on the 30th day of the storage period.

### 3.12. Sensory evaluation

When comparing the control and other nanoemulsions (C-1 and C-2), it was observed that kiwifruit samples treated with C-3 exhibited a noteworthy distinction ( $P < 0.05$ ) in overall acceptability on the final day of shelf life. The control kiwi samples scored 4.5 on the hedonic scale, suggesting a strong aversion. By contrast, C-1, C-2, and C-3 received ratings of 6.0 (indicating a moderate level of acceptance), 6.4 (indicating a moderate level of liking), and 7.5 (indicating a high level of liking), respectively. The texture ratings of kiwifruit varied substantially across the treatments (C-1, C-2, and C-3) and the control group. Furthermore, there was a notable disparity in the texture of C-3 on the last day of its shelf life. The control kiwi samples were rated 4.0 on the hedonic scale, indicating a severe aversion. Conversely, C-1, C-2, and C-3 were rated as 5.0 (moderately disliked), 5.5 (somewhat liked), and 6.5 (liked) accordingly. The application of C-3 coatings had a notable influence on kiwifruits' structural integrity and texture. The C-3 coatings had the highest level of acceptance in terms of flavor, surpassing other

coatings. Among the several coatings tested, the C-3 coatings exhibited the most pronounced effect on kiwifruit samples. The control kiwi samples received a rating of 4.5 on the hedonic scale, suggesting a significant level of disapproval. By comparison, C-1, C-2, and C-3 received ratings of 6.0 (just about acceptable), 6.4 (average preference), and 7.5 (liked), respectively. The assessment of kiwifruit's visual characteristics and pigmentation demonstrated a mutually dependent connection. The judges determined that the C-3 variety remained captivating, whereas the control group was despised due to the intense aroma and odor resulting from elevated quantities of ethylene and gaseous emissions. The main reason for the hate of control is its visual appearance and hue. The coatings C-2 and C-3 performed well, with C-3 showing a significant advantage ( $p > 0.05$ ) due to its higher barrier qualities.

### 3.13. Correlation plot analysis

The correlation analysis demonstrates strong relationships among these traits, as illustrated in Fig. 6b, offering valuable insights into their interrelated nature. The data reveals a robust positive correlation (0.96) between weight loss and decay incidence in kiwifruit samples, suggesting a direct association where greater weight loss is linked to

elevated levels of decay. These findings indicate that weight loss has a significant effect on deterioration. A strong and constant positive relationship exists between total suspended solids (TSS) and decay incidence, maturity index, ethylene output, and bacterial count. Elevated amounts of suspended particles can impact these quality indicators, potentially compromising the overall quality of the fruit and its shelf life.

On the other hand, titratable acidity shows strong negative associations with several characteristics. Elevated titratable acidity levels can enhance the preservation of fruit quality by reducing decay, weight loss, suspended particles, maturity index, ethylene production, and bacterial count. Firmness demonstrates notable inverse associations with various characteristics, except titratable acidity (Fig. 4b).

The findings indicate a correlation between reduced firmness and increased rates of weight loss, decay incidence, suspended particles, maturity index, ethylene production, and bacterial count. The findings emphasize the need for firmness in maintaining excellent attributes. Furthermore, substantial correlations exist between the bacterial count and decay incidence, suspended solids, and maturity index, indicating that changes influence the bacterial count in these parameters. The findings provide crucial insights into the possible impacts of nano-emulsions on the quality parameters of kiwifruit. Weight loss is a feature that can occur in fruits due to moisture loss. This can have a detrimental impact on the fruit's integrity and make it more prone to deterioration. Greater weight loss is correlated with increased vulnerability, leading to potential entry points for infections, which is connected with a higher incidence of decay. A significant correlation exists between the number of bacteria and the occurrence of degradation and suspended particles. High levels of bacteria suggest strong microbial activity, which could lead to degradation and affect other quality aspects.

#### 4. Conclusion

The research findings suggest that the application of nano-emulsified coatings C-1, C-2, and C-3, derived from carboxymethyl cellulose combined with thyme, clove, and cardamom essential oils, significantly enhances the kiwifruit's shelf life during storage. The examination of these coatings unveiled distinguishable nanostructures and chemical

interactions. It has been noted that the coatings significantly reduce ethylene generation, decay occurrence, weight loss, and bacterial population. Moreover, they have been discovered to enhance the kiwifruit's hardness, titratable acidity, and maturity index. Notably, C-3, characterized by higher quantities of essential oils, exhibited improved preservation advantages. The discovery implies that utilizing nanoemulsion coatings infused with essential oils could enhance the postharvest quality and extend the shelf life of kiwifruit. The latest work has demonstrated the potential of integrating multiphase essential oils into carboxymethylcellulose nanoemulsions (C-1, C-2, and C-3) for food preservation. This can be linked to their exceptional and significant potential.

#### Author statement

The author confirms sole responsibility for the following: study conception and design, data collection, analysis and interpretation of results, and manuscript preparation.

#### CRediT authorship contribution statement

**Shahzad Zafar Iqbal:** Writing – review & editing, Writing – original draft, Visualization, Supervision, Resources, Project administration, Methodology, Funding acquisition, Conceptualization. **Ali Haider:** Writing – original draft, Methodology, Formal analysis, Data curation. **Fazal ur Rehman:** Writing – review & editing, Supervision. **Guizhuo Cui:** Writing – review & editing, Software. **Muhammad Waseem:** Visualization, Resources. **Munawar Iqbal:** Writing – review & editing. **Amin Mousavi Khaneghah:** Writing – review & editing, Conceptualization.

#### Declaration of competing interest

The authors declare that they have no known competing financial interests or personal relationships that could have appeared to influence the work reported in this paper.

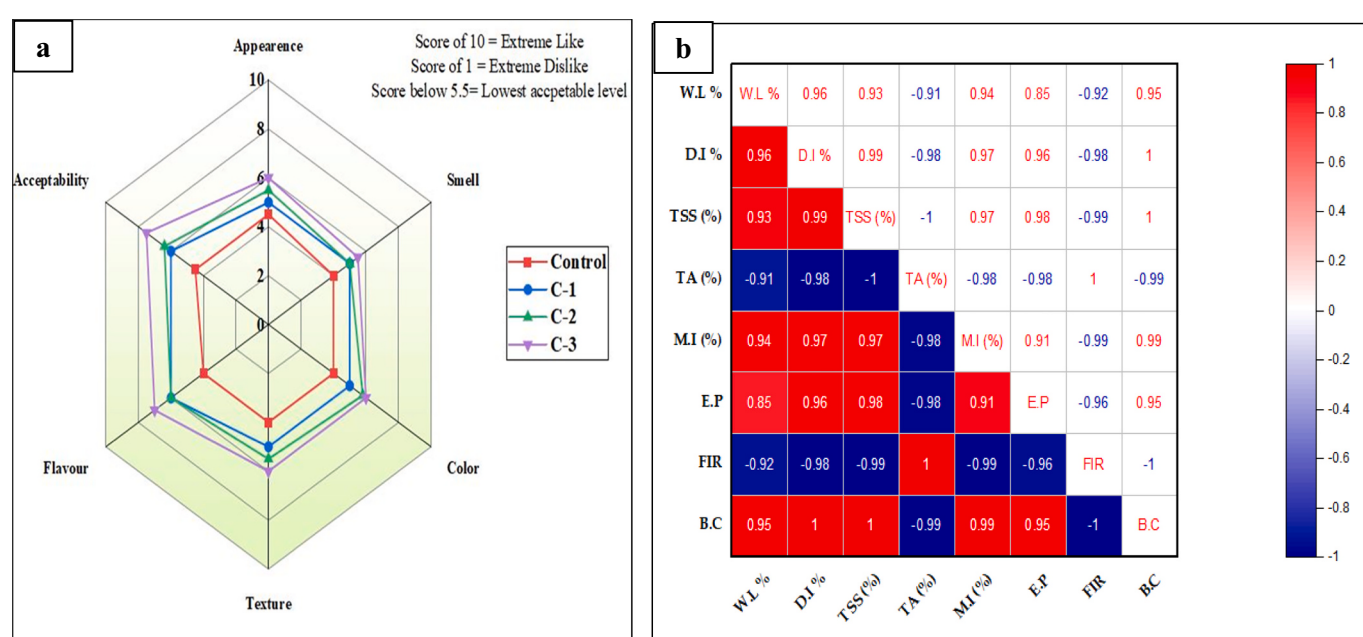


**Fig. 7.** The graphical representation of sensory evaluations (smell, color, flavor, texture, appearance, and acceptability) in comparison of control and nanoemulsions (C-1, C-2, and C-3), treated kiwifruit sample (a); Correlation analysis among quality parameters of kiwifruit samples (b).

Abbreviations: W.L % = weigh loss %; D.I = decay incidence (%); TSS = Total suspended solids (%); T.A (%) = titratable acidity; M.I (%) = maturity index (%); E.P = ethylene production; FIR = firmness; B.C = bacterial count

## Data availability

Data will be made available on request.

## Acknowledgement

The author (Iqbal, S.Z.) appreciates the financial assistance of the Higher Education Commission Islamabad, grant no NRPU-5574.

## References

- [1] J. Xu, L. Zhou, J. Miao, W. Yu, L. Zou, W. Zhou, C. Liu, W. Liu, Effect of cinnamon essential oil nanoemulsion combined with ascorbic acid on enzymatic browning of cloudy apple juice, *Food Bioproc. Tech.* 13 (2020) 860–870.
- [2] G. Yıldız, G. Yıldız, M.R. Khan, R.M. Aadil, High-intensity ultrasound treatment to produce and preserve the quality of fresh-cut kiwifruit, *Journal of Food Processing and Preservation* 46 (5) (2022) e16542.
- [3] S. Beirão-da-Costa, A. Steiner, L. Correia, J. Empis, M. Moldão-Martins, Effects of maturity stage and mild heat treatments on quality of minimally processed kiwifruit, *J. Food Eng.* 76 (4) (2006) 616–625.
- [4] L. Fu, S. Liu, F. Xu, Effect of treatment with MeJA on physiology and biochemistry in blueberry fruit, *Journal of Shenyang Normal University (Natural Science Edition)* 35 (2017) 473–475.
- [5] L. Mao, J. Jeong, F. Que, D.J. Huber, Physiological properties of fresh-cut watermelon (*Citrullus lanatus*) in response to 1-methylcyclopropene and post-processing calcium application, *J. Sci. Food Agric.* 86 (1) (2006) 46–53.
- [6] F.B. Meng, Z.Z. Gou, Y.C. Li, L.H. Zou, W.J. Chen, D.Y. Liu, The efficiency of lemon essential oil-based nanoemulsions on the inhibition of *Phomopsis* sp. and reduction of postharvest decay of kiwifruit, *Foods* 11 (10) (2022) 1510.
- [7] X. Shan, F. Xu, Effects of preservation at low temperature on physiological quality of postharvest sweet corn, *Journal of Shenyang Normal University (Natural Science Edition)* 33 (2015) 507–510.
- [8] R.C. Soliva-Fortuny, O. Martín-Belloso, New advances in extending the shelf-life of fresh-cut fruits: a review, *Trends Food Sci. Technol.* 14 (9) (2003) 341–353.
- [9] A. Yadav, N. Kumar, A. Upadhyay, A. Singh, R.K. Anurag, R. Pandiselvam, Effect of mango kernel seed starch-based active edible coating functionalized with lemongrass essential oil on the shelf-life of guava fruit, *Quality Assurance and Safety of Crops & Foods* 14 (3) (2022) 103–115.
- [10] F.M. Allai, Z. Azad, B. Dar, K. Gul, Effect of extrusion processing conditions on the techno-functional, antioxidant, textural properties and storage stability of wholegrain-based breakfast cereal incorporated with Indian horse chestnut flour, *Italian Journal of Food Science* 34 (3) (2022) 105–123.
- [11] B. Nurhadi, S. Selly, S. Nurhasanah, R.A. Saputra, H.R. Arifin, The virgin coconut oil (VCO) emulsion powder characteristics: effect of Pickering emulsion with microcrystalline cellulose (MCC) and different drying techniques, *Italian Journal of Food Science* 34 (1) (2022) 67–85.
- [12] S.Z. Tesfay, L.S. Magwaza, Evaluating the efficacy of moringa leaf extract, chitosan and carboxymethyl cellulose as edible coatings for enhancing quality and extending postharvest life of avocado (*Persea americana mill.*) fruit, *Food Packag. Shelf Life* 11 (2017) 40–48.
- [13] H.S. El-Sayed, S.M. El-Sayed, A.M. Mabrouk, G.A. Nawwar, A.M. Youssef, Development of eco-friendly probiotic edible coatings based on chitosan, alginate and carboxymethyl cellulose for improving the shelf life of UF soft cheese, *J. Polym. Environ.* 29 (2021) 1941–1953.
- [14] H. Togrul, N. Arslan, Extending shelf-life of peach and pear by using CMC from sugar beet pulp cellulose as a hydrophilic polymer in emulsions, *Food Hydrocolloids* 18 (2) (2004) 215–226. Xu, F., Liu, S., Liu, Y., Xu, J., Liu, T., & Dong, S. (2019). Effectiveness of lysozyme coatings and 1-MCP treatments on storage and preservation of kiwifruit. *Food Chemistry*, 288, 201–207.
- [15] S.K. Das, K. Vishakha, S. Das, D. Chakraborty, A. Ganguli, Carboxymethyl cellulose and cardamom oil in a nanoemulsion edible coating inhibit the growth of foodborne pathogens and extend the shelf life of tomatoes, *Biocatal. Agric. Biotechnol.* 42 (2022) 102369.
- [16] Z. Deng, K. Zhu, R. Li, L. Zhou, H. Zhang, Cellulose nanocrystals incorporated  $\beta$ -chitosan nanoparticles to enhance the stability and in vitro release of  $\beta$ -galactosidase, *Food Res. Int.* 137 (2020) 109380.
- [17] Y. Bai, T. Qiu, B. Chen, C. Shen, C. Yu, Z. Luo, H. Zhang, Formulation and stabilization of high internal phase emulsions: stabilization by cellulose nanocrystals and gelatinized soluble starch, *Carbohydr. Polym.* 312 (2023) 120693.
- [18] G.A.D. Vichakshana, D.J. Young, W.S. Choo, Extraction, purification, food applications, and recent advances for enhancing the bioavailability of 6-gingerol from ginger—a review, *Quality Assurance and Safety of Crops & Foods* 14 (4) (2022) 67–83.
- [19] S. Siripongvutikorn, C. Klubpet, C. Anantapan, V. Seechamnuntarakit, Some factors affecting the bioactive substances of lactogenic tea, *Italian Journal of Food Science* 35 (3) (2023) 75–89.
- [20] S.B.S. Arunasalam, N. Karthikeyan, A. Thangaiah, R. Balasubramanian, A. Thiagarajan, R. Jacob, Active compound analysis of ethanolic extract of roselle calyxes (*Hibiscus sabdariffa L.*), *Quality Assurance and Safety of Crops & Foods* 15 (2) (2023) 117–128.
- [21] M. Ishfaq, W. Hu, Z. Hu, Y. Guan, R. Zhang, A review of nutritional implications of bioactive compounds of ginger (*Zingiber officinale Roscoe*), their biological activities and nano-formulations, *Italian Journal of Food Science* 34 (3) (2022) 1–12.
- [22] S.A. Wani, H.R. Naik, J.A. Wagay, N.A. Ganje, M.Z. Mulla, B.N. Dar, Menthā: a review on its bioactive compounds and potential health benefits, *Quality Assurance and Safety of Crops & Foods* 14 (4) (2022) 154–168.
- [23] H. Jafarizadeh-Malmiri, N. Anarjan, A. Berenjian, Developing three-component ginger-cinnamon-cardamom composite essential oil nanoemulsion as natural food preservatives, *Environ. Res.* 204 (2022) 112133.
- [24] L. Wang, M. Yu, S. Ding, J. Cao, X. Meng, L. Li, M. Sun, Zebrafish models for the evaluation of essential oils (EOs): a comprehensive review, *Quality Assurance and Safety of Crops & Foods* 15 (4) (2023) 156–178.
- [25] A.I. Gavrila, C.G. Chisega-Negrila, L. Maholea, M.L. Gavrila, O.C. Părvulescu, I. Popa, Enhancing the extraction process efficiency of thyme essential oil by combined ultrasound and microwave techniques, *Agronomy* 13 (9) (2023) 2331.
- [26] A. Guenbour, M. Taleb, S. Boukhriß, H. Oudda, Theoretical and Experimental Inhibitory Properties of Mild Steel in Phosphoric Acid by Clove Essential Oil, 2018.
- [27] L. De Fátima Ferreira Da Silva, R.B. Pallaoro, E.M. De Freitas, L. Hoehne, D. Heidrich, E.M. Ethur, Antibacterial activity of *Lithraea molleoides* hook et Arn. and *Poiretia latifolia* Vogel essential oils combined with gentamicin on foodborne disease-causing bacteria, *Biocatalysis and Agricultural Biotechnology* 48 (2023) 102620.
- [28] N. Khodaei, M. Houde, S. Bayen, S. Karboune, Exploring the synergistic effects of essential oil and plant extract combinations to extend the shelf life and the sensory acceptance of meat products: multi-antioxidant systems, *Journal of Food Science and Technology* 60 (2) (2022) 679–691.
- [29] R. Pathania, R. Kausik, M.A. Khan, Essential oil nanoemulsions and their antimicrobial and food applications, *Current Research in Nutrition and Food Science Journal* 6 (3) (2018) 626–643.
- [30] A. Acevedo-Fani, R. Soliva-Fortuny, O. Martín-Belloso, Nanoemulsions as edible coatings, *Curr. Opin. Food Sci.* 15 (2017) 43–49.
- [31] A. Prakash, R. Baskaran, V. Vadivel, Citral nanoemulsion incorporated edible coating to extend the shelf life of fresh-cut pineapples, *LWT* 118 (2020) 108851.
- [32] R. Kumar, G. Ghoshal, M. Goyal, Moth bean starch (*Vigna aconitifolia*): isolation, characterization, and development of edible/biodegradable films, *J. Food Sci. Technol.* 56 (2019) 4891–4900.
- [33] Z. Rao, X. Lei, Y. Chen, J. Ling, J. Zhao, J. Ming, Facile fabrication of robust bilayer film loaded with chitosan active microspheres for potential multifunctional food packing, *Int. J. Biol. Macromol.* 231 (2023) 123362.
- [34] C. Du, S. Li, Y. Fan, Y. Lu, J. Sheng, Y. Song, Preparation of gelatin-chitosan bilayer film loaded citral nanoemulsion as pH and enzyme stimuli-responsive antibacterial material for food packaging, *Int. J. Biol. Macromol.* 254 (2024) 127620.
- [35] L. Nian, M. Wang, Y. Zeng, J. Jiang, S. Cheng, C. Cao, Modified HKUST-1-based packaging with ethylene adsorption property for food preservation, *Food Hydrocoll.* 135 (2023) 108204.
- [36] D.M. Beckles, Factors affecting the postharvest soluble solids and sugar content of tomato (*Solanum lycopersicum L.*) fruit, *Postharvest Biology and Technology* 63 (1) (2012) 129–140.
- [37] M. Miranda, M.D.M.M. Ribeiro, P.C. Spricigo, L. Pilon, M.C. Mitsuyuki, D. S. Correa, M.D. Ferreira, Carnauba wax nanoemulsion applied as an edible coating on fresh tomato for postharvest quality evaluation, *Heliyon* 8 (7) (2022) e09803.
- [38] J. Yun, X. Fan, X. Li, T.Z. Jin, X. Jia, J.P. Mattheis, Natural surface coating to inactivate *Salmonella enterica* serovar *Typhimurium* and maintain quality of cherry tomatoes, *Int. J. Food Microbiol.* 193 (2015) 59–67.
- [39] M.A. Rojas-Graü, M.S. Tapia, O. Martín-Belloso, Using polysaccharide-based edible coatings to maintain quality of fresh-cut Fuji apples, *LWT-Food Sci. Technol.* 41 (1) (2008) 139–147.
- [40] S. Escrivano, A. Lopez, H. Sivertsen, W.V. Biasi, A.J. Macnish, E.J. Mitcham, Impact of 1-methylcyclopropene treatment on the sensory quality of 'Bartlett' pear fruit, *Postharvest Biology and Technology* 111 (2016) 305–313.
- [41] V. Ghosh, S. Saranya, A. Mukherjee, N. Chandrasekaran, Cinnamon oil nanoemulsion formulation by ultrasonic emulsification: investigation of its bactericidal activity, *J. Nanosci. Nanotechnol.* 13 (1) (2013) 114–122.
- [42] S. Noori, F. Zeynali, H. Almasi, Antimicrobial and antioxidant efficiency of nanoemulsion-based edible coating containing ginger (*Zingiber officinale*) essential oil and its effect on safety and quality attributes of chicken breast fillets, *Food Control* 84 (2018) 312–320.
- [43] L.-J. Yin, B.-S. Chu, I. Kobayashi, M. Nakajima, Performance of selected emulsifiers and their combinations in the preparation of  $\beta$ -carotene nano-dispersions, *Food Hydrocoll.* 23 (6) (2009) 1617–1622.
- [44] C. Arancibia, R. Navarro-Lisboa, R.N. Zúñiga, S. Matiacevich, Application of CMC as thickener on nanoemulsions based on olive oil: physical properties and stability, *International Journal of Polymer Science* 2016 (2016) 6280581.
- [45] L.T. Cuba-Chiem, L. Huynh, J. Ralston, D.A. Beattie, In situ particle film ATR FTIR spectroscopy of carboxymethyl cellulose adsorption on talc: binding mechanism, pH effects, and adsorption kinetics, *Langmuir* 24 (15) (2008) 8036–8044.
- [46] M.S. Yeasmin, M.I.H. Mondal, Synthesis of highly substituted carboxy-methyl cellulose depending on cellulose particle size, *Int. J. Biol. Macromol.* 80 (2015) 725–731.
- [47] N. Habibi, Preparation of biocompatible magnetite-carboxymethyl cellulose nanocomposite: characterization of nanocomposite by FTIR, XRD, FESEM and TEM, *Spectrochim. Acta A Mol. Biomol. Spectrosc.* 131 (2014) 55–58.
- [48] A.H. Saputra, L. Qadhyana, A.B. Pitaloka, Synthesis and characterization of carboxymethyl cellulose (CMC) from water hyacinth using ethanol-isobutyl alcohol mixture as the solvents, *International Journal of Chemical Engineering and Applications* 5 (1) (2014) 36.

- [49] Y. Chu, T. Xu, C. Gao, X. Liu, N. Zhang, X. Feng, X. Liu, X. Shen, X. Tang, Evaluations of physicochemical and biological properties of pullulan-based films incorporated with cinnamon essential oil and Tween 80, *Int. J. Biol. Macromol.* 122 (2019) 388–394.
- [50] D. Muscat, M.J. Tobin, Q. Guo, B. Adhikari, Understanding the distribution of natural wax in starch–wax films using synchrotron-based FTIR (S-FTIR), *Carbohydr. Polym.* 102 (2014) 125–135.
- [51] C.K. Saurabh, S. Gupta, P.S. Variyar, A. Sharma, Effect of addition of nanoclay, beeswax, tween-80 and glycerol on physicochemical properties of guar gum films, *Ind. Crop. Prod.* 89 (2016) 109–118.
- [52] H. Liu, R. Adhikari, Q. Guo, B. Adhikari, Preparation and characterization of glycerol plasticized (high-amylose) starch–chitosan films, *J. Food Eng.* 116 (2) (2013) 588–597.
- [53] Q.-P. Zhong, W.-S. Xia, Physicochemical properties of edible and preservative films from chitosan/cassava starch/gelatin blend plasticized with glycerol, *Food Technol. Biotechnol.* 46 (3) (2008) 262–269.
- [54] A.M. Abdullah, S.B. Aziz, M. Brza, S.R. Saeed, B.A. Al-Asbahi, N.M. Sadiq, A.A. A. Ahmed, A.R. Murad, Glycerol as an efficient plasticizer to increase the DC conductivity and improve the ion transport parameters in biopolymer based electrolytes: XRD, FTIR and EIS studies, *Arab. J. Chem.* 15 (6) (2022) 103791.
- [55] H. Almasi, B. Ghanbarzadeh, A.A. Entezami, Physicochemical properties of starch–CMC–nanoclay biodegradable films, *Int. J. Biol. Macromol.* 46 (1) (2010) 1–5.
- [56] F. Hasani, A. Pezeshki, H. Hamishehkar, Effect of surfactant and oil type on size droplets of betacarotene-bearing nanoemulsions, *Int. J. Curr. Microbiol. App. Sci.* 4 (9) (2015) 146–155.
- [57] S. Manzoor, A. Gull, S.M. Wani, T.A. Ganaie, F.A. Masoodi, K. Bashir, A.R. Malik, B. N. Dar, Improving the shelf life of fresh cut kiwi using nanoemulsion coatings with antioxidant and antimicrobial agents, *Food Biosci.* 41 (2021) 101015.
- [58] X. Hu, G. Zhou, C. Wang, Z. Bo, Research of alginate and lysozyme compound coating on fresh-keeping of cherry tomatoes, *Food and Fermentation Industries* 37 (10) (2011) 193–196.
- [59] M. Mostaghimi, M. Majdinasab, S.M.H. Hosseini, Characterization of alginate hydrogel beads loaded with thyme and clove essential oils nanoemulsions, *J. Polym. Environ.* (2022) 1–15.
- [60] J. Burdon, P. Pidakala, P. Martin, D. Billing, H. Boldingh, Fruit maturation and the soluble solids harvest index for ‘Hayward’ kiwifruit, *Sci. Hortic.* 213 (2016) 193–198.
- [61] T.M. da Silva, R. Briano, C. Peano, N.R. Giuggioli, The use of a new explanatory methodology to assess maturity and ripening indices for kiwiberry (*Actinidia arguta*): preliminary results, *Postharvest Biol. Technol.* 163 (2020) 111122.
- [62] H.P.C. Kumarhami, Y.-H. Kim, Y.-B. Kwack, J. Kim, J.G. Kim, Application of chitosan as edible coating to enhance storability and fruit quality of kiwifruit: a review, *Sci. Hortic.* 292 (2022) 110647.
- [63] J. Chai, Y. Wang, Y. Liu, K. Yong, Z. Liu, 1-MCP extends the shelf life of ready-to-eat ‘Hayward’ and ‘Qihong’ kiwifruit stored at room temperature, *Sci. Hortic.* 289 (2021) 110437.
- [64] Q. Ma, Y. Cong, J. Wang, C. Liu, L. Feng, K. Chen, Pre-harvest treatment of kiwifruit trees with mixed culture fermentation broth of *Trichoderma pseudokoningii* and *Rhizopus nigricans* prolonged the shelf life and improved the quality of fruit, *Postharvest Biology and Technology* 162 (2020) 111099.
- [65] H. Yan, R. Wang, N. Ji, S. Cao, C. Ma, J. Li, G. Wang, Y. Huang, J. Lei, L. Ba, Preparation, shelf, and eating quality of ready-to-eat “Guichang” kiwifruit: regulation by ethylene and 1-MCP, *Front. Chem.* 10 (2022) 934032.
- [66] A. Guerreiro, C. Gago, D. Passos, J. Martins, S.P. Cruz, F. Veloso, R. Guerra, M. D. Antunes, Enhancing the Storability of Hardy Kiwifruit (*Actinidia arguta* cv. ‘Ken’s Red’) with Edible Coatings during Postharvest Handling, 2023.
- [67] S. Jung, Y. Cui, M. Barnes, C. Satam, S. Zhang, R.A. Chowdhury, A. Adumbumkulath, O. Sahin, C. Miller, S.M. Sajadi, Multifunctional bio-nanocomposite coatings for perishable fruits, *Adv. Mater.* 32 (26) (2020) 1908291.
- [68] G. Sortino, P. Inglese, V. Farina, R. Passafiume, A. Allegra, The use of *Opuntia ficus-indica* mucilage and *Aloe arborescens* as edible coatings to improve the physical, chemical, and microbiological properties of ‘Hayward’ kiwifruit slices, *Horticulturae* 8 (3) (2022) 219.